🔓**Open Access**

Switchable Multi-Wavelength Thulium-Doped Fiber Laser Using Four-Mode Fiber Based Sagnac Loop Filter

Ying Guo
Fengping Yan
Ting Feng
Luna Zhang
Qi Qin
Wenguo Han
Zhuoya Bai
Hong Zhou
Yuping Suo
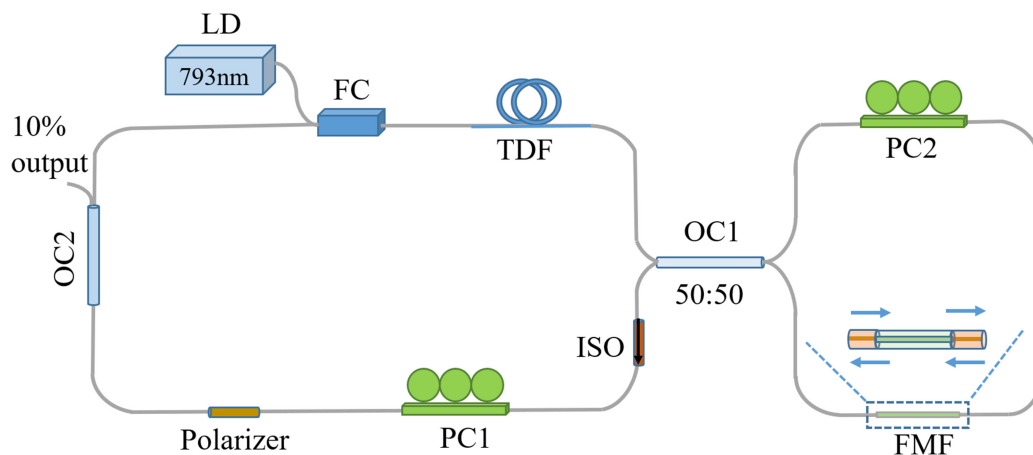
Switchable Multi-Wavelength Thulium-Doped Fiber Laser Using Four-Mode Fiber Based Sagnac Loop Filter

Ying Guo [iD],[1,2] Fengping Yan [iD],[1] Ting Feng [iD],[3] Luna Zhang [iD],[1] Qi Qin [iD],[1] Wenguo Han,[1] Zhuoya Bai,[1] Hong Zhou,[4] and Yuping Suo[5]

[1]Key Laboratory of All Optical Network and Advanced Telecommunication Network, Ministry of Education, Institute of Lightwave Technology, Beijing Jiaotong University, Beijing 100044, China
[2]College of Science, Zhongyuan University of Technology, Zhengzhou 450007, China
[3]Photonics Information Innovation Center, Hebei Provincial Center for Optical Sensing Innovations, College of Physics Science & Technology, Hebei University, Baoding 071002, China
[4]Department of Electronics, Information and Communication Engineering, Osaka Institute of Technology, Asahi-ku, Osaka 535-8585, Japan
[5]Shanxi Provincial People's Hospital, Shanxi Medical University, Taiyuan 030012, China

Abstract: A switchable multi-wavelength thulium-doped fiber laser (TDFL) using a four-mode fiber based Sagnac loop filter was proposed and demonstrated. The Sagnac loop, incorporating a 4.8 m long four-mode step-index fiber, acting as a comb filter was analyzed theoretically and experimentally. By adjusting two polarization controllers, eight stable single-wavelength operations and five stable dual-wavelength operations were obtained with easy switching between the different operation modes. The wavelength range covered during the single-wavelength switchable operation with a signal-to-noise ratio of up to 55 dB was ∼28.51 nm. In dual-wavelength switchable operation, the maximum and minimum wavelength spacings were ∼21.78 nm and ∼1.50 nm, respectively. Due to the abundant wavelength resources, the proposed TDFL has great potential in wavelength division multiplexing free-space optical communications, optical fiber sensing, and photonic generation of microwave signals.

Index Terms: Four-mode fiber, thulium-doped fiber laser (TDFL).

1. Introduction

Lasers in the 2-μm band are particularly important because they operate in the atmospheric transmission window and in the human eye safety band. Various thulium-doped fiber lasers (TDFLs) such as Q-switched TDFL [1], mode-locked TDFL [2], [3], multi-wavelength TDFL [4]–[7], and narrow linewidth TDFL [8]–[10] are currently available, and, among these, the multi-wavelength TDFL has attracted intense research attention in recent years, since the multi-wavelength fiber

lasers have the great potential in a wide range of applications, for instance, gas spectroscopy [11], fiber sensing [12], wavelength division multiplexing systems [13], and photonic generation of microwave signals [14].

To date, various comb filters such as two cascaded Sagnac loops [15], a Sagnac loop incorporating two-stage polarization maintaining fibers [16], a Sagnac loop combining a multimode interference filter [17], a micro-fiber-optic Fabry–Perot interferometer (FPI) [18], a non-adiabatic tapered fiber [19], and sampled fiber Bragg gratings [20] have been proposed for achieving 2-μm band multi-wavelength lasing output in TDFLs. Recently, the few-mode fiber has attracted much attention due to its many applications such as mode-division multiplex (MDM) transmission systems [21], tunable fiber lasers [22], and fiber sensors [23], [24]. In particular, switchable multi-wavelength fiber lasers in 1.55-μm band based on few-mode fibers have been studied extensively [25]–[29]. For example, Zhou *et al.* reported a switchable multi-wavelength erbium-doped fiber laser (EDFL) based on a four-mode fiber Bragg grating. This laser can be switched among the operation states of single-, dual-, and triple-wavelength operations [25]. Sun *et al.* reported a triple-wavelength switchable EDFL based on a few-mode high-birefringence fiber [26], [27], and Yang *et al.* reported a five-wavelength switchable EDFL based on a few-mode fiber Bragg grating [28]. However, the switchable multi-wavelength TDFL using the few-mode fiber based interferometer filter was rarely reported.

Generally, multi-wavelength fiber laser output in 2-μm band can be easily obtained using a multi-mode fiber optical interferometer. For example, Zhang *et al.* reported triple-wavelength laser operation based on a single-mode–multi-mode–single-mode (SMS) fiber Mach–Zehnder interferometer (MZI) structure [30], while Daniel *et al.* reported a simple technique for transverse mode selection in a large-mode-area (multi-mode) fiber laser, and achieved a single-spatial-mode output beam [31]. However, compared to using a multi-mode fiber in an interferometer, the use of a few-mode fiber in an interferometer filter can provide a more clear, simple and regular output interference spectrum, and enable easy determination and tuning of the periods and peak wavelengths of the multi-channel filter for meeting the requirements of different applications. To date, multi-wavelength lasing in a TDFL using a few-mode fiber has been only explored in a study performed by Wang *et al.* who designed a 2-μm switchable dual-wavelength fiber laser using a cascaded filter structure based on a few-mode fiber-embedded dual-channel MZI and the spatial mode beating effect [32]. Unfortunately, in their study, only two lasing wavelengths were obtained for switchable operation and the wavelength-spacing in dual-wavelength operation cannot be changed flexibly.

In this work, a switchable multi-wavelength TDFL using a four-mode fiber based Sagnac loop (FMF-SL) filter was proposed and demonstrated. Our approach exploited the use of an FMF-SL as a comb filter that was also analyzed theoretically, and a polarization-dependent loss component was introduced to suppress the mode competition. By adjusting the polarization state of light inside the ring cavity, the TDFL can output single-, dual- and triple-wavelength lasers. Because the clear free spectral range (FSR) of the FMF-SL filter is only 0.75 nm, the number of the multi-wavelength operation states available for our TDFL is rather high, and the covered wavelength range of switchable operations is wider than that of most reported multi-wavelength TDFLs [32], [33]. The optical signal-to-noise ratios (OSNRs) obtained for the proposed TDFL are higher than that reported by Wang *et al.* [32]. Furthermore, our laser also has the advantages of a simpler structure and greater operational flexibility.

2. Experimental Setup, Theory and Principle

The experimental structure of the proposed switchable multi-wavelength TDFL using an FMF-SL filter is shown in Fig. 1. A 1.75-m-long commercial double-cladding thulium-doped fiber (TDF) produced by Nufern Cor. with a core/cladding diameter of 10/130 μm is used as the active fiber. The TDF is pumped by a 793 nm laser diode (LD) through a 793/2000 nm fiber combiner (FC) with the maximum output power of 12 W. To ensure unidirectional oscillation, an isolator (ISO) is applied. A polarizer is used to enforce the linear polarization of the light propagation in the ring cavity. Meanwhile, a polarization controller (PC), PC1, combined with the polarizer is used as the
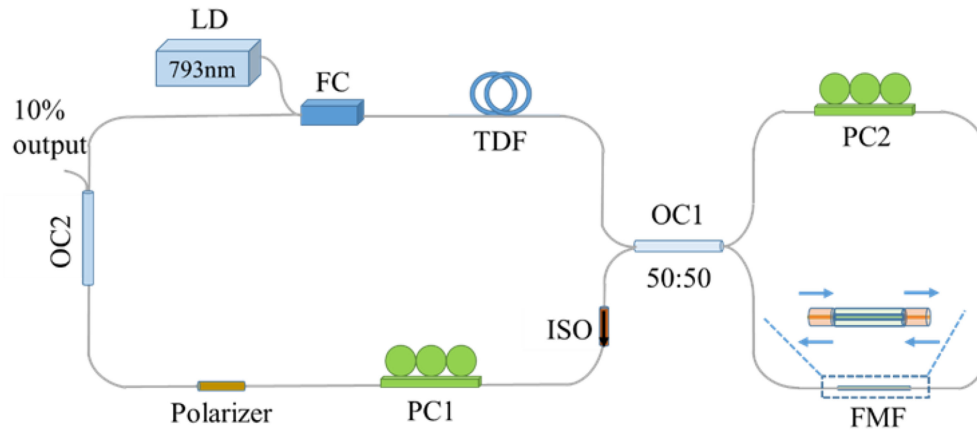
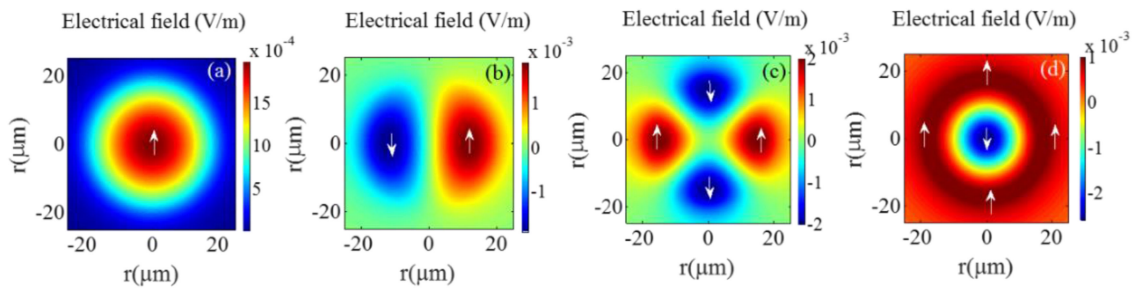Fig. 1. Experimental structure of the proposed switchable multi-wavelength TDFL using an FMF-SL filter.

Fig. 2. Guiding optical mode in FMF. (a) LP_{01}, (b) LP_{11}, (c) LP_{21}, and (d) LP_{02} modes. The arrows indicate the polarization directions.

polarization-dependent loss component [34], [35]. The FMF-SL shown in the right panel of Fig. 1 is approximately 7 m long and consists of a 4.8-m-long four-mode step-index fiber (YOFC: SI-4) with a core/cladding diameter of 19/125 μm, a 2.2-m-long single mode fiber (SMF) which is the pigtailed fiber of the other PC, PC2, and an optical coupler (OC1) with a coupling ratio of 50/50. The left loop with a length of approximately 7.75 m includes the TDF with the length of 1.75 m and an SMF with the length of 6 m which is the pigtailed fiber of the ISO, PC1, polarizer, and the other OC (OC2) with a coupling ratio of 90/10. The length of the entire laser cavity is approximately 14.75 m. An optical spectrum analyzer (YOKOGAWA AQ6375, OSA) with a resolution of 0.05 nm is adopted to receive 10% output power from the laser cavity for measurement.

As shown in Fig. 1, the four-mode fiber (FMF) in the Sagnac loop is sandwiched by two SMFs. The four transverse modes in FMF are the LP_{01}, LP_{11}, LP_{21} and LP_{02} modes. Figures 2(a)-(d) show the transverse electrical field distributions of the four modes, respectively, obtained from the mode analysis in the entire cross-section of the fiber using the finite difference method with a grid accuracy of 10^{-3} nm [36] and implemented using the MATLAB software. At the boundary of the materials with the different refractive index values, the tangential component of the electric field and the normal component of the electric flux are continuous. At the center of the fiber, the condition of $\bar{\Psi}|_{r\to0}= 0$, $(d\bar{\Psi})/(dr)|_{r=0}= 0$ is satisfied, where Ψ is the electrical field, and r is the spatial coordinate. It is observed that unlike the LP_{11} and LP_{21} modes, the LP_{01} and LP_{02} modes have circumferentially symmetric distributions. Therefore, if the SMF and FMF are connected with core-center alignment, only the LP_{01} and LP_{02} modes can be selectively excited upon light propagation from the SMF into the FMF [37]. Since the LP_{01} and LP_{02} modes have
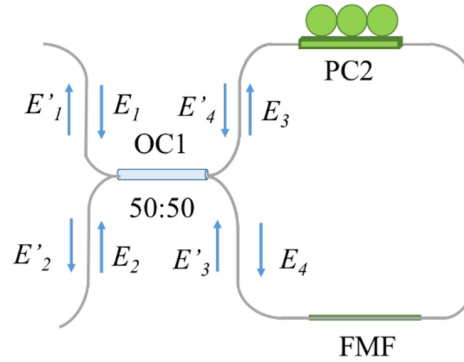
Fig. 3. Structure of FMF-SL.

different effective refractive index values (1.44548 and 1.44425, respectively), with the difference of $\Delta n_{eff} \approx 1.2 \times 10^{-3}$ in the 2-μm band, the FMF acts as two different channels for transmission in a manner very similar to that of a high-birefringence fiber. Consequently, the use of the FMF in the Sagnac loop enables it act as a comb filter.

The transmission characteristics of the proposed filter can be analyzed by the Jones matrix representation, where $\begin{pmatrix} \cos\theta & \sin\theta \\ -\sin\theta & \cos\theta \end{pmatrix}$, $\begin{pmatrix} e^{-j\varphi_1} & 0 \\ 0 & e^{j\varphi_1} \end{pmatrix}$, $\begin{pmatrix} \sqrt{1-s} & j\sqrt{s} \\ j\sqrt{s} & \sqrt{1-s} \end{pmatrix}$ are the matrices of the PC2, the FMF and the OC1, respectively. θ is the deflection angle of the PC, and φ is the phase difference caused by the fast- and slow-axial components transmitting in the FMF. According to the structure shown in Fig. 3, the transmission equations are as given as

$$\begin{pmatrix} E_3 \\ E_4 \end{pmatrix} = \begin{pmatrix} \sqrt{1-s} & j\sqrt{s} \\ j\sqrt{s} & \sqrt{1-s} \end{pmatrix} \begin{pmatrix} E_1 \\ E_2 \end{pmatrix}, \tag{1}$$

$$E_3' = \begin{pmatrix} e^{-j\varphi_1} & 0 \\ 0 & e^{j\varphi_1} \end{pmatrix} \begin{pmatrix} \cos\theta & \sin\theta \\ -\sin\theta & \cos\theta \end{pmatrix} E_3, \tag{2}$$

$$E_4' = \begin{pmatrix} \cos\theta & \sin\theta \\ -\sin\theta & \cos\theta \end{pmatrix} \begin{pmatrix} e^{-j\varphi_1} & 0 \\ 0 & e^{j\varphi_1} \end{pmatrix} E_4, \tag{3}$$

$$\begin{pmatrix} E_1' \\ E_2' \end{pmatrix} = \begin{pmatrix} \sqrt{1-s} & j\sqrt{s} \\ j\sqrt{s} & \sqrt{1-s} \end{pmatrix} \begin{pmatrix} E_4' \\ E_3' \end{pmatrix}. \tag{4}$$

We define the power of input light as P_0 and the power of transmitted light as P_2, and we have

$$P_2 = \left| E_2' \right|^2. \tag{5}$$

Based on the Sagnac interference principle [38], the transmission spectrum is described by

$$t = P_2/P_0 = (1-2s) + 4s(1-s)\sin^2\theta\cos^2\varphi, \tag{6}$$

where $\varphi = \pi \Delta n_{eff} L/\lambda$, s is the split ratio of the optical coupler, L is the length of the FMF, λ is the transmission wavelength, and Δn_{eff} is the difference between the effective refractive index values of the propagating modes. Therefore, the free spectral range (FSR) is given by:

$$\Delta\lambda = \lambda^2/(L\Delta n_{eff}). \tag{7}$$

As observed from Fig. 3, the input beams are transmitted forward and backward in the FMF-SL filter and their polarizations can be rotated by adjusting PC2. Due to the use of the FMF, the propagation phases of the beams are different when they are recombined at the OC1, so that the
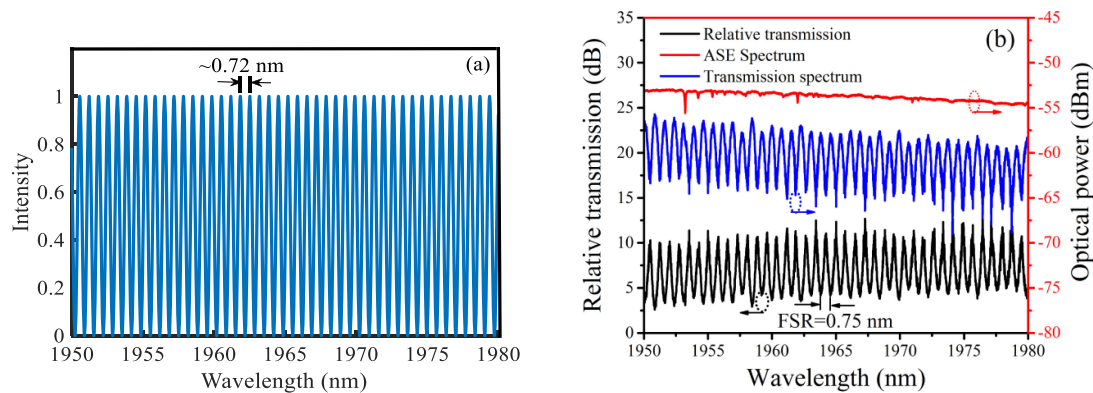
Fig. 4. (a) Simulated transmission spectra of the FMF-SL filter, (b) amplified spontaneous emission spectrum of the 2 m double-cladding TDF (red), transmission spectrum (blue) and relative transmission spectrum (black) of the FMF-SL filter.

beams interfere with each other [26]. Using Eq. (6), we calculated the transmission spectrum of the FMF-SL filter for $s = 0.5$, $\theta = \pi/2$, and the obtained results are displayed in Fig. 4(a), showing an FSR of ~0.72 nm. The FMF-SL was characterized by using a TDF amplifier and the OSA. The relative transmission spectrum of the FMF-SL filter was obtained by subtracting the transmission spectrum of the FMF-SL filter from the amplified spontaneous emission (ASE) spectrum, and is shown in Fig. 4(b). It is observed that the FSR value is ~0.75 nm, in good agreement with the simulated result. The uneven spectral envelope observed in Fig. 4(b) arises mainly from the effect of the other two modes in FMF that were not suppressed sufficiently, and may lead to an uneven multi-wavelength lasing output in the proposed TDFL.

3. Experimental Results and Discussion

The principle of wavelength switchable operation can be explained as follows. Due to the use of the polarizer and the PCs, polarization dependent loss can be brought in for the lasing wavelengths. Only the lasing wavelength with the polarization direction parallel to the operating axis of the polarizer has the lowest loss and oscillates in the laser cavity finally, enabling the single-wavelength operation. Furthermore, by carefully adjusting the two PCs, a power-equalizer can be established, based on the nonlinear polarization rotation (NPR) effect [35], [39], that is driven by the PC1, PC2 and the polarizer. This can significantly suppress the competition among the lasing modes and hence the dual-wavelength or multi-wavelength operations can be obtained successfully.

In the experiment, when the pump power was fixed at 2.69 W, stable single wavelength operation was obtained by adjusting PC1 and PC2, which was induced by a balance between the gain and loss in the laser cavity. We achieved switchable operation among eight single-wavelength lasers at 1948.86, 1954.86, 1958.55, 1963.86, 1966.13, 1969.77, 1971.28 and 1977.37 nm, respectively. The wavelength covering range was ~28.51 nm, and the wavelength spacing between any two lasers were the integer multiples of the FSR of the FMF-SL filter. As observed from Fig. 5, the minimum OSNR is ~46 dB and the maximum OSNR is ~55 dB, mainly due to the uneven transmission spectrum envelope of the FMF-SL filter. To demonstrate output stability, the lasing wavelength of 1956.96 nm was tested over 60 min with no adjustment to any part of the fiber laser applied during the measurement. The obtained output spectra are shown in Fig. 6(a), and the fluctuations of the central wavelength and output power are shown in Fig. 6(b). It is observed from Fig. 6(b) that the power variation was less than ±0.23 dB, and no obvious wavelength drift was observed at the resolution of 0.05 nm of the OSA over 60 min at room temperature. This indicates that our TDFL can operate stably in single-wavelength lasing.
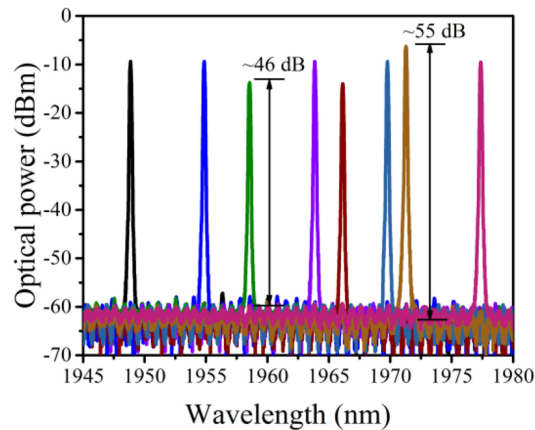
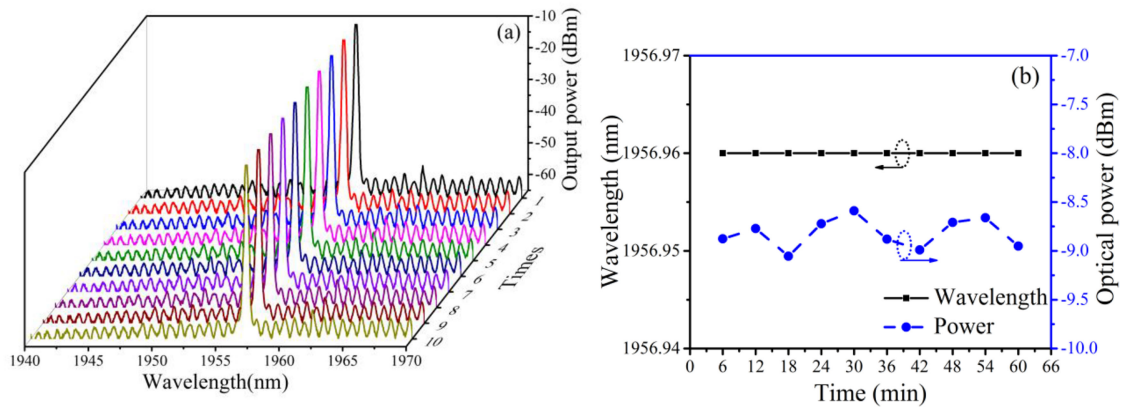Fig. 5. Output spectra of switchable single wavelength lasing.

Fig. 6. (a) Measurement of the output spectra for ten times OSA scans with the time interval of six minutes, (b) fluctuations of the center wavelength and output power, respectively.

In addition, dual-wavelength lasing was obtained and switched by adjusting the PCs. As shown in Fig. 7(a), the dual-wavelength operation lasing was carried out at 1958.58 and 1960.08 nm, for the spacing between the two lasing wavelengths of 1.50 nm, which is twice larger than the FSR of the FMF-SL filter. The peak power difference is ~0.71 dB, and both lasers have an OSNR of ~40 dB. As shown in Fig. 7(b), the dual-wavelength output was then switched to lase at 1950.34 nm and 1958.60 nm, and in this case, the spacing between the two wavelengths 8.26 nm is 11 times larger than the FSR of the FMF-SL filter. The peak power difference was ~1.41 dB and was mainly due to the uneven transmission spectrum envelope of the FMF-SL filter. OSNR values of ~43 dB were obtained for both lasing wavelengths.

When the pump power was fixed at 3.08 W, five different wavelength spacings were obtained for dual-wavelength operation by the appropriate rotation of the three plates of PC1 and PC2. As shown in Fig. 8, the five wavelength spacings were 6.02 (lasing at 1948.86 and 1954.88 nm), 6.77 (lasing at 1962.28 and 1969.05 nm), 14.33 (lasing at 1957.85 and 1972.18 nm), 15.78 (lasing at 1954.88 and 1970.66 nm), and 21.78 (lasing at 1948.87 and 1970.65 nm), and OSNRs of ~45 dB were obtained for all five spacings. The OSNRs were higher than that of 35 dB reported by Wang *et al.* [32]. The maximum and minimum output power differences of the two lasing wavelengths among these five cases were 2.83 dB and 1.16 dB, respectively. Note that, the stable dual-wavelength
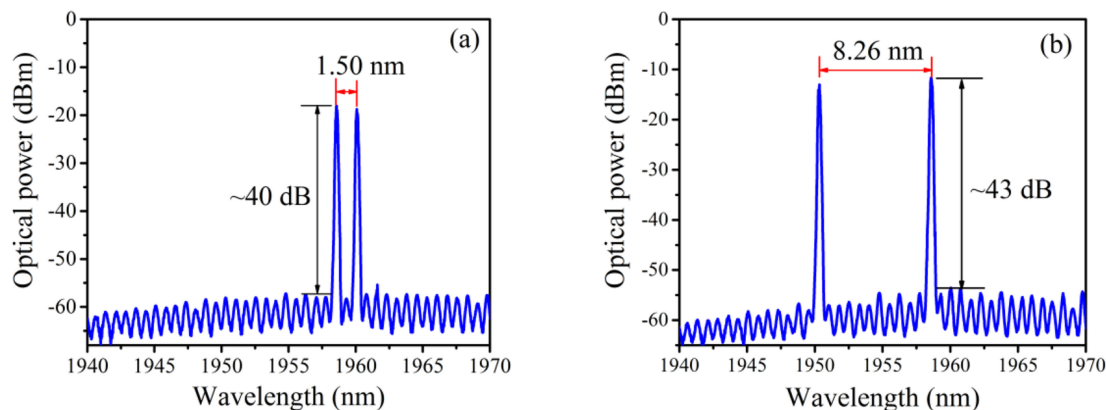
Fig. 7. Dual-wavelength operation with different spacings. (a) 1.5 nm, (b) 8.26 nm.
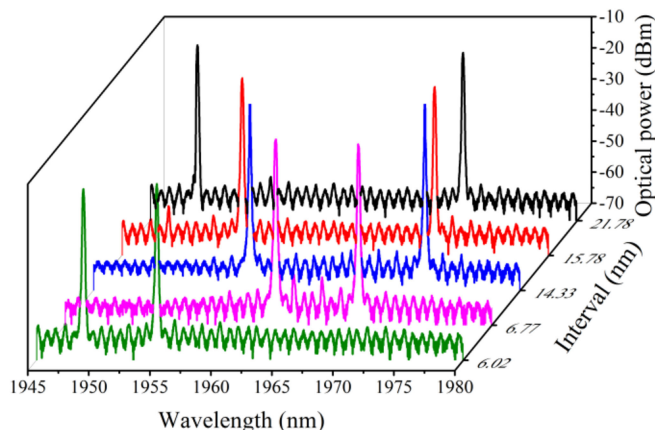

Fig. 8. Output spectra of five different dual-wavelength operations.

operations with different spacings were obtained depending on the extent of mode competition suppressing of the gain-equalizer aforementioned, on one hand, and the uneven spectral envelope of FMF-SL observed in Fig. 4(b), on the other hand.

To demonstrate the stability of dual-wavelength operation, the output spectra were measured at room temperature over 30 min for the wavelength interval of 6.08 nm (lasing at 1948.86 and 1954.88 nm), with the measured spectra shown in Fig. 9(a). As shown in Figs. 9(b) and 9(c), the wavelength drifts were both less than ±0.01 nm, and the power variations were less than ±1.30 dB and ±1.39 dB, respectively in the 30-min duration of the experiment. Although the wavelength and power fluctuations were larger than those in single-wavelength operation due to the stronger wavelength competition in TDF for the two lasers oscillating simultaneously, these results verify that the TDFL is also stable in dual-wavelength operation. The maximum and minimum output power differences of the two lasing lines were 1.48 dB and 0.02 dB, respectively.

Furthermore, triple-wavelength lasing output was also achieved as demonstrated in Fig. 10 by adjusting PCs, with the three wavelengths located at 1948.86, 1954.88, and 1970.66 nm. Due to the external environmental disturbance and particularly the severe internal mode competition, the triple-wavelength operation did not show satisfactory stability. Therefore, other stabilizing mechanisms should be introduced into the laser cavity to obtain stable multi-wavelength lasing.
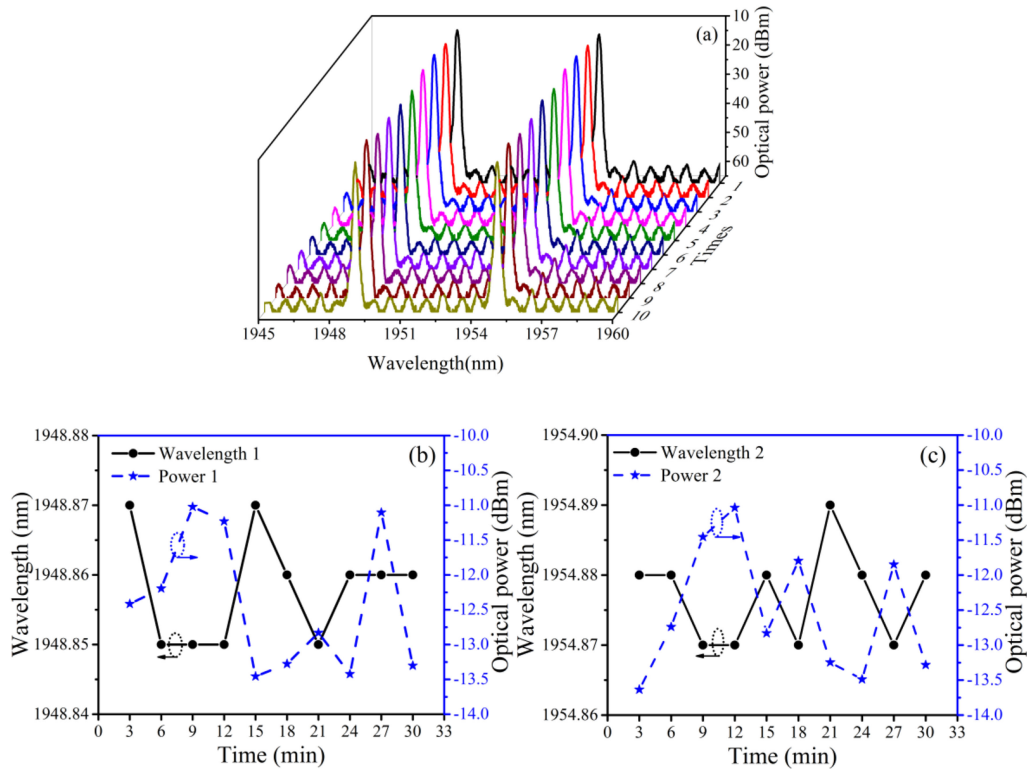
Fig. 9. (a) Measurement of the output spectra for ten times OSA scans with a time interval of 3 min, (b) fluctuations of the center wavelength 1 and output power 1 at 1948.86 nm, (c) fluctuations of the center wavelength 2 and output power 2 at 1954.88 nm.
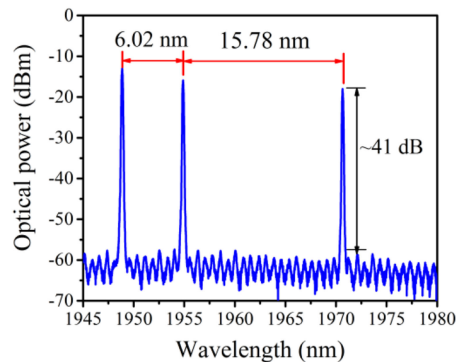

Fig. 10. Spectrum of triple-wavelength lasing.

Unfortunately, this will lead to the greater complexity of the laser system that may be unfavorable for the high output performance in single- or dual-wavelength operation.

4. Conclusion

In conclusion, a switchable multi-wavelength TDFL based on an FMF-SL filter was proposed and demonstrated experimentally. A Sagnac loop containing an FMF with the length of 4.8 m was used as the comb filter, and the FSR was found to be ∼0.75 nm both theoretically and experimentally. The high stability of the TDFL was realized by introducing polarization-dependent loss inside the

laser cavity. By tuning the PCs used in the device, the laser output could be switched among eight stable single-wavelength operations covering a wavelength range of ∼28.51 nm, and also could be switched among five stable dual-wavelength operations with a maximum spacing of ∼21.78 nm. In addition, the experimentally-demonstrated TDFL has potential for triple-wavelength lasing operation. Regardless of the operation wavelength, the OSNR of the TDFL was larger than 40 dB. We believe that the performance of the proposed fiber laser can be improved further if good vibration isolation and temperature-stabilization techniques are used in practical applications. The proposed TDFL may be applied in various fields such as optical fiber sensing and laser medicine.

References

[1] A. S. Sharbirin, H. Ahmad, and M. F. Ismail, "Q-switched thulium-doped fiber laser at 1860 nm and 1930 nm using a Holmium-doped fiber as an amplified spontaneous emission filter," *Opt. Laser Technol.*, vol. 123, 2020, Art. no. 105908.

[2] S. Liu, F.-P. Yan, L.-N. Zhang, W.-G. Han, Z.-Y. Bai, and H. Zhou, "Noise-like femtosecond pulse in passively mode-locked Tm-doped NALM-based oscillator with small net anomalous dispersion," *J. Opt.*, vol. 18, 2015, Art. no. 015508.

[3] X. Liu, F. Li, X. Yu, S. Zhang, and Y. Tang, "High-pulse-energy mode-locked and Q-switched large-mode-area thulium fiber laser," *Opt. Commun.*, vol. 457, 2020, Art. no. 124730.

[4] M. F. B. Ismail, M. Dernaika, A. Khodaei, S. W. Harun, and H. Ahmad, "Tunable dual-wavelength thulium-doped fiber laser at 1.8 μm region using spatial-mode beating," *J. Modern Opt.*, vol. 62, pp. 892–896, 2015.

[5] S. Liu, F. Yan, W. Peng, T. Feng, Z. Dong, and G. Chang, "Tunable dual-wavelength thulium-doped fiber laser by employing a HB-FBG," *IEEE Photon. Technol. Lett.*, vol. 26, pp. 1809–1812, 2014.

[6] W. Peng, F. Yan, Q. Li, S. Liu, T. Feng, and S. Tan, "A 1.97 μm multiwavelength thulium-doped silica fiber laser based on a nonlinear amplifier loop mirror," *Laser Phys. Lett.*, vol. 10, 2013, Art. no. 115102.

[7] L. Zhang *et al.*, "Switchable multi-wavelength Thulium-doped fiber laser employing a polarization-maintaining sampled fiber bragg grating," *IEEE Access*, vol. 7, pp. 155437–155445, 2019.

[8] T. Feng, F. Yan, S. Liu, Y. Bai, W. Peng, and S. Tan, "Switchable and tunable dual-wavelength single-longitudinal-mode erbium-doped fiber laser with special subring-cavity and superimposed fiber Bragg gratings," *Laser Phys. Lett.*, vol. 11, 2014, Art. no. 125106.

[9] X. Xiao *et al.*, "3 W narrow-linewidth ultra-short wavelength operation near 1707 nm in thulium-doped silica fiber laser with bidirectional pumping," *Appl. Phys. B*, vol. 123, 2017, Art. no. 135.

[10] F. Yan, W. Peng, S. Liu, T. Feng, Z. Dong, and G. Chang, "Dual-wavelength single-longitudinal-mode Tm-doped fiber laser using PM-CMFBG," *IEEE Photon. Technol. Lett.*, vol. 27, no. 9, pp. 951–954, May 2015.

[11] J. Marshall, G. Stewart, and G. Whitenett, "Design of a tunable L-band multi-wavelength laser system for application to gas spectroscopy," *Meas. Sci. Technol.*, vol. 17, pp. 1023–1031, 2006.

[12] K. Venkataraayan, S. Askraba, K. E. Alameh, and C. L. Smith, "Multi-wavelength laser sensor for intruder detection and discrimination," *Opt. Lasers Eng.*, vol. 50, pp. 176–181, 2012.

[13] A. E. H. Oehler, S. C. Zeller, K. J. Weingarten, and U. Keller, "Broad multiwavelength source with 50 GHz channel spacing for wavelength division multiplexing applications in the telecom C band," *Opt. Lett.*, vol. 33, pp. 2158–2160, 2008.

[14] C. Xiangfei, D. Zhichao, and Y. Jianping, "Photonic generation of microwave signal using a dual-wavelength single-longitudinal-mode fiber ring laser," *IEEE Trans. Microw. Theory Techn.*, vol. 54, no. 2, pp. 804–809, Feb. 2006.

[15] L. Zhu, W. He, M. Dong, X. Lou, and F. Luo, "Tunable multi-wavelength thulium-doped fiber laser incorporating two-stage cascaded Sagnac loop comb filter," *Modern Phys. Lett. B*, vol. 30, 2016, Art. no. 1650292.

[16] W. He, L. Zhu, M. Dong, and F. Luo, "Tunable and switchable thulium-doped fiber laser utilizing Sagnac loops incorporating two-stage polarization maintaining fibers," *Opt. Fiber Technol.*, vol. 29, pp. 65–69, 2016.

[17] W. Ma *et al.*, "Wavelength-spacing switchable dual-wavelength single longitudinal mode thulium-doped fiber laser at 1.9 μm," *IEEE Photon. J.*, vol. 8, no. 6, Dec. 2016, Art. no. 1504508.

[18] M. Wang, Y. Huang, L. Yu, Z. Song, D. Liang, and S. Ruan, "Multiwavelength thulium-doped fiber laser using a micro fiber-optic fabry–perot interferometer," *IEEE Photon. J.*, vol. 10 no. 4, Aug. 2018, Art. no. 1502808.

[19] A. W. Al-Alimi, M. H. Abu Bakar, N. H. Zainol Abidin, A. F. Abas, M. T. Alresheedi, and M. A. Mahdi, "Dual-wavelength thulium-doped fiber laser assisted by non-adiabatic tapered fiber," *Opt. Laser Technol.*, vol. 112, pp. 26–29, 2019.

[20] L. Zhang *et al.*, "Wavelength-tunable thulium-doped fiber laser with sampled fiber Bragg gratings," *Opt. Laser Technol.*, vol. 120, 2019, Art. no. 105707.

[21] S. H. Chang *et al.*, "Mode- and wavelength-division multiplexed transmission using all-fiber mode multiplexer based on mode selective couplers," *Opt. Express*, vol. 23, pp. 7164–7172, 2015.

[22] Y. Qi *et al.*, "Wavelength-switchable fiber laser based on few-mode fiber filter with core-offset structure," *Opt. Laser Technol.*, vol. 81, pp. 26–32, 2016.

[23] T. Huang, S. Fu, S. Liu, M. Tang, and D. Liu, "Discrimination between temperature and strain using fiber Bragg grating inscribed in few-mode silica-germanate fiber," in *Proc. OptoElectron. Commun. Conf. Australian Conf. Opt. Fiber Technol.*, 2014, pp. 1058–1060.

[24] J. Su, X. Dong, and C. Lu, "Intensity detection scheme of sensors based on the modal interference effect of few mode fiber," *Measurement*, vol. 79, pp. 182–187, 2016.

[25] Y. Zhou, P. Gao, X. Zhang, P. Wang, L. Chen, and W. Gao, "Switchable multi-wavelength erbium-doped fiber laser based on a four-mode FBG," *Chin. Opt. Lett.*, vol. 17, 2019, Art. no. 010604.

[26] G. Sun, Y. Zhou, Y. Hu, and Y. Chung, "Switchable erbium-doped fiber ring laser based on Sagnac loop mirror incorporating few-mode high birefringence fiber," *Opt. Commun.*, vol. 284, pp. 1608–1611, 2011.

[27] G. Sun, Y. Zhou, L. Cui, and Y. Chung, "Polarization controlled multiwavelength switchable erbium-doped fiber laser based on high birefringence few-mode fiber loop mirror," *Laser Phys.*, vol. 21, pp. 1914–1918, 2011.

[28] K. Yang *et al.*, "Five-wavelength-switchable all-fiber erbium-doped laser based on few-mode tilted fiber Bragg grating," *Opt. Laser Technol.*, vol. 108, pp. 273–278, 2018.

[29] G. Sun, Y. Zhou, Y. Hu, and Y. Chung, "Broadly tunable fiber laser based on merged sagnac and intermodal interferences in few-mode high-birefringence fiber loop mirror," *IEEE Photon. Technol. Lett.*, vol. 22, no. 11, pp. 766–768, Jun. 2010.

[30] P. Zhang, T. Wang, W. Ma, K. Dong, and H. Jiang, "Tunable multiwavelength Tm-doped fiber laser based on the multimode interference effect," *Appl. Opt.*, vol. 54, pp. 4667–4671, May 2015.

[31] J. M. O. Daniel, J. S. P. Chan, J. W. Kim, J. K. Sahu, M. Ibsen, and W. A. Clarkson, "Novel technique for mode selection in a multimode fiber laser," *Opt. Exp.*, vol. 19, pp. 12434–12439, 2011.

[32] S. Wang, P. Lu, S. Zhao, D. Liu, W. Yang, and J. Zhang, "2-μm switchable dual-wavelength fiber laser with cascaded filter structure based on dual-channel Mach–Zehnder interferometer and spatial mode beating effect," *Appl. Phys. B*, vol. 117, pp. 563–569, 2014.

[33] X. Ma, S. Luo, and D. Chen, "Switchable and tunable thulium-doped fiber laser incorporating a Sagnac loop mirror," *Appl. Opt.*, vol. 53, pp. 4382–4385, 2014.

[34] A. A. Latiff, H. Shamsudin, Z. C. Tiu, H. Ahmad, and S. W. Harun, "Switchable soliton mode-locked and multi-wavelength operation in thulium-doped all-fiber ring laser," *J. Nonlinear Opt. Phys. Mater.*, vol. 25, 2016, Art. no. 1650034.

[35] C. Jia, X. Liang, M. Rochette, and L. R. Chen, "Alternate wavelength switching in a widely tunable dual-wavelength Tm^{3+}-doped fiber laser at 1900 nm," *IEEE Photon. J.*, vol. 7, no. 4, Aug. 2015, Art. no. 1502907.

[36] Y.-C. Lu, L. Yang, W.-P. Huang, and S.-S. Jian, "Improved full-vector finite-difference complex mode solver for optical waveguides of circular symmetry," *J. Lightw. Technol.*, vol. 26, no. 13, pp. 1868–1876, Jul. 2008.

[37] A. Kumar, N. K. Goel, and R. K. Varshney, "Studies on a few-mode Fiber-Optic Strain Sensor based on LP01-LP02 Mode Interference," *J. Lightw. Technol.*, vol. 19, no. 3, pp. 358–362, Mar. 2001.

[38] G. C. H. MA and C. Feng, "A cascaded comb filter based on Sagnac interferometer," *Opt. Fiber Elect. Cable Appl.*, vol. 01, pp. 28–32, 2011.

[39] Z. Zhang, L. Zhan, K. Xu, J. Wu, Y. Xia, and J. Lin, "Multiwavelength fiber laser with fine adjustment, based on nonlinear polarization rotation and birefringence fiber filter," *Opt. Lett.*, vol. 33, pp. 324–326, 2008.